

# Novel $\alpha$ -Oxoamide Advanced-Glycation Endproducts within the $N^6$ -Carboxymethyl Lysine and $N^6$ -Carboxyethyl Lysine Reaction Cascades

Tim Baldensperger,<sup>†</sup> Tobias Jost,<sup>†</sup> Alexander Zipprich,<sup>‡</sup> and Marcus A. Glomb<sup>\*,†</sup>

<sup>†</sup>Institute of Chemistry, Food Chemistry, Martin-Luther-University Halle-Wittenberg, Kurt-Mothes-Strasse 2, 06120 Halle/Saale, Germany

<sup>‡</sup>Department of Internal Medicine I, Martin-Luther-University Halle-Wittenberg, Ernst-Grube-Strasse 40, 06120 Halle/Saale, Germany

**ABSTRACT:** The highly reactive  $\alpha$ -dicarbonyl compounds glyoxal and methylglyoxal are major precursors of posttranslational protein modifications in vivo. Model incubations of  $N^2$ -*t*-Boc-lysine and either glyoxal or methylglyoxal were used to further elucidate the underlying mechanisms of the  $N^6$ -carboxymethyl lysine and  $N^6$ -carboxyethyl lysine reaction cascades. After independent synthesis of the authentic reference standards, we were able to detect  $N^6$ -glyoxylyl lysine and  $N^6$ -pyruvoyl lysine for the first time by HPLC-MS<sup>2</sup> analyses. These two novel amide advanced-glycation endproducts were exclusively formed under aerated conditions, suggesting that they were potent markers for oxidative stress. Analogous to the well-known Strecker degradation pathway, leading from amino acids to Strecker acids, the oxidation of an enaminol intermediate is suggested to be the key mechanistic step. A highly sensitive workup for the determination of AGEs in tissues was developed. In support of our hypothesis, the levels of  $N^6$ -glyoxylyl lysine and  $N^6$ -pyruvoyl lysine in rat livers indeed correlated with liver cirrhosis and aging.

**KEYWORDS:** Maillard reaction, amide advanced-glycation endproducts, methylglyoxal, glyoxal, oxidative stress, aging

## INTRODUCTION

Louis-Camille Maillard described the nonenzymatic browning reaction of reducing sugars and amines upon heating in 1912. Already at this early stage, he postulated the reaction's great importance in the physiology and pathology of humans on the basis of the wide availability of carbohydrates and amines.<sup>1</sup> Starting in the 1940s, Maillard-reaction research focused not only on the formation of colors, aromas, and tastes in food<sup>2</sup> but also on the negative side-effects, like the formation of foodborne toxins, such as acrylamide.<sup>3</sup> In addition, Maillard reactions are widely accepted as an important source of reactive intermediates that lead to advanced-glycation endproducts (AGEs) in vivo. AGEs are stable posttranslational protein modifications and were correlated with the development and progression of various chronic and age-related pathologies. As an example, the levels of the most abundant AGE,  $N^6$ -carboxymethyl lysine (CML), increased with the severity of diabetes<sup>4</sup> and rose in an almost linear fashion with age in human lens proteins.<sup>5</sup>

Because of the progress in analytical methods, the understanding of Maillard-reaction mechanisms has strongly improved in recent years. Highly reactive  $\alpha$ -dicarbonyl compounds, like glyoxal (GO), methylglyoxal (MGO), and deoxyglucosones, have been identified as key intermediates and quantitated in order to understand the chemistry of AGE formation in vitro and in vivo.<sup>6–10</sup> These precursors are transformed to the stable endproducts mainly by three different mechanisms under physiological conditions:<sup>9</sup> oxidative  $\alpha$ -dicarbonyl cleavage,<sup>11</sup> amine-induced  $\beta$ -dicarbonyl cleavage,<sup>12</sup> and isomerization.<sup>13</sup> Rather-long-chained dicarbonyl structures, for example, 1-deoxyglucosone and 2,3-diketogulonic acid, tend

to fragment by oxidative  $\alpha$ -dicarbonyl cleavage and amine-induced  $\beta$ -dicarbonyl cleavage, resulting in mixtures of short-chained carbonyls, carboxylic acids, and their corresponding amide AGEs.<sup>14,15</sup> On the other hand, two of the quantitatively most relevant AGEs, CML and  $N^6$ -carboxyethyl lysine (CEL), are formed nonoxidatively by isomerization after a reaction between protein-bound lysines and the short-chained dicarbonyl structures GO and MGO, respectively. Alternative products formed in the complex reaction cascades include monovalent AGEs with an amide structure, like  $N^6$ -glycoloyl lysine (GALA) and  $N^6$ -lactoyl lysine, and cross-linking compounds, like the glyoxal lysine amide (GOLA) and the glyoxal lysine dimer (GOLD).<sup>9</sup>

It is important to understand that in contrast to all the other structures identified so far within this mechanistic scheme, only CML can be formed by additional oxidative pathways. A main route was shown to proceed via the direct oxidative fragmentation of the Amadori product of lysine and glucose, although the exact mechanism is still lacking. In addition, multiple minor reaction pathways have been published, mainly related to the formation of glyoxal or glycolaldehyde from higher sugars via, for example, the metal-catalyzed autooxidation of glucose or the amine-catalyzed single-electron transfers of pyrazinium-radical cations within the Namiki pathway.<sup>16</sup> Consequently, CML has been used as a marker of oxidative stress in diabetes, for example, which is generally characterized

Received: December 11, 2017

Revised: January 29, 2018

Accepted: February 6, 2018

by increases in both carbonyls and oxidative stress, accelerating the formation of late-stage complications.<sup>17</sup> However, because of the multiple routes leading to CML formation, the value of CML as a suitable chemical parameter for oxidative stress has to be challenged. The present work therefore successfully aimed to identify two novel AGEs specific for oxidation within the isomerization-reaction cascade and test their applicability in vivo.

## MATERIALS AND METHODS

**Chemicals.** All chemicals of the highest quality available were provided by Sigma-Aldrich (Munich/Steinheim, Germany), Fluka (Taufkirchen, Germany), Merck (Darmstadt, Germany), Roth (Karlsruhe, Germany) and Sigma (Taufkirchen, Germany), unless otherwise indicated. The NMR solvents were purchased from ARMAR Chemicals (Leipzig/Doettingen, Germany).

The standard reference substances CML,<sup>7</sup> GALA,<sup>13</sup> CEL,<sup>18</sup> and N<sup>6</sup>-lactoyl lysine<sup>12</sup> as well as the Amadori product of glucose and N<sup>2</sup>-*t*-Boc-lysine,<sup>7</sup> N<sup>2</sup>-*t*-Boc-lysine *t*-butyl ester (1),<sup>19</sup> glyoxylic acid diethyl acetal (2),<sup>20</sup> and pyruvic acid *N,N*-dimethyl hydrazone (4)<sup>21</sup> were synthesized according to the literature.

**N<sup>2</sup>-*t*-Boc-N<sup>6</sup>-(2,2-diethoxy acetyl) Lysine *t*-Butyl Ester (3).** Compound 2 (647 mg, 4.37 mmol) and hydroxybenzotriazole (HOBt, 590 mg, 4.37 mmol) were dissolved in 10 mL of dry THF under an argon atmosphere at 0 °C. After 10 min, 745 mg (4.8 mmol) of 1-ethyl-3-(3-(dimethylamino)propyl)carbodiimide (EDC) was added. A solution of 1.319 g (4.37 mmol) of 1 in 5 mL of dry THF was added dropwise after 20 min. The reaction mixture was warmed to room temperature and stirred for 16 h. The solvent was evaporated under a vacuum, and the residue was dissolved in 10 mL of EtOAc and washed with a saturated NaHCO<sub>3</sub> solution and brine (10 mL each). The organic layer was dried over Na<sub>2</sub>SO<sub>4</sub> and the solvents were evaporated. The crude product was purified by column chromatography on a silica gel 60 using hexane–acetone (3:1). Fractions containing 3 (TLC: R<sub>f</sub> 0.35 in hexane–acetone (3:1), ninhydrin detection) were collected, concentrated in vacuo and dried under a high vacuum to afford compound 3 as a yellow viscous oil (633 mg, 34%). <sup>1</sup>H NMR (400 MHz, MeOH-*d*<sub>4</sub>): δ (ppm) = 1.23 (t, <sup>3</sup>J = 7.1 Hz, 6H), 1.44 (s, 9H), 1.46 (s, 9H), 1.38 (m, 2H), 1.56 (m, 2H), 1.75 (m, 2H), 3.22 (t, <sup>3</sup>J = 7.0 Hz, 2H), 3.61 (m, 4H), 3.93 (t, <sup>3</sup>J = 5.0 Hz, 1H), 4.79 (s, 1H). <sup>13</sup>C NMR (100 MHz, MeOH-*d*<sub>4</sub>): δ (ppm) = 15.4, 24.3, 28.3, 28.8, 30.0, 32.7, 39.8, 55.8, 63.4, 99.7, 158.2, 170.4, 173.8. HR-MS: *m/z* 433.2900 (found); *m/z* 433.2908 (calcd for C<sub>21</sub>H<sub>41</sub>O<sub>7</sub>N<sub>2</sub> [M + H]<sup>+</sup>).

**N<sup>6</sup>-Glyoxylyl Lysine.** Compound 3 (178 mg, 0.41 mmol) was dissolved in acetone and 6 M HCl (10 mL each). After being stirred for 30 min, the mixture was diluted with 100 mL of water and concentrated to a volume of approximately 20 mL under a vacuum. After being washed with 20 mL of EtOAc, the aqueous phase was separated and evaporated to dryness. The crude product was purified by column chromatography on a Lichroprep RP C18 using water–methanol (9:1). Fractions with positive ninhydrin detections (TLC: R<sub>f</sub> 0.14 in water–butanol–acetic acid (8:1:1)) were collected, evaporated, and lyophilized to afford N<sup>6</sup>-glyoxylyl lysine as an amorphous material (75 mg, 90%). <sup>1</sup>H NMR (400 MHz, D<sub>2</sub>O): δ (ppm) = 1.34 (m, 2H), 1.48 (m, 2H), 1.85 (m, 2H), 3.13 (t, <sup>3</sup>J = 7.0 Hz, 2H), 3.96 (t, <sup>3</sup>J = 6.5 Hz, 1H), 5.15 (s, 1H). <sup>13</sup>C NMR (100 MHz, D<sub>2</sub>O): δ (ppm) = 21.4, 27.7, 29.3, 38.5, 52.7, 86.7, 172.0, 172.1. HR-MS: *m/z* 203.1028 (found); *m/z* 203.1026 (calcd for C<sub>8</sub>H<sub>13</sub>O<sub>4</sub>N<sub>2</sub> [M + H]<sup>+</sup>).

**N<sup>2</sup>-*t*-Boc-N<sup>6</sup>-pyruvoyl Lysine *t*-Butyl Ester (5).** Compound 4 (590 mg, 4.54 mmol) and HOBt (613 mg, 4.54 mmol) were dissolved in 10 mL of dry THF under an argon atmosphere at 0 °C. After 10 min, 775 mg (5.0 mmol) of EDC was added. A solution of 1.369 g (4.54 mmol) of 1 in 5 mL of dry THF was added dropwise after 20 min. The reaction mixture was warmed to room temperature and stirred for 16 h. The solvent was evaporated under a vacuum, and the residue was dissolved in 10 mL of EtOAc and washed with saturated NaHCO<sub>3</sub> solution and brine (10 mL each). The organic layer was dried over Na<sub>2</sub>SO<sub>4</sub> and solvents were evaporated. The crude product was

purified by column chromatography on a silica gel 60 using hexane–acetone (3:1). Fractions containing 5 (TLC: R<sub>f</sub> 0.22 in hexane–acetone (3:1), ninhydrin detection) were collected, concentrated in vacuo, and dried under a high vacuum to afford compound 5 as a yellow viscous oil (841 mg, 50%). As described by Katayama, the *N,N*-dimethyl hydrazone protective group was removed by silica-gel purification.<sup>22</sup> <sup>1</sup>H NMR (400 MHz, MeOH-*d*<sub>4</sub>): δ (ppm) = 1.44 (s, 9H), 1.46 (s, 9H), 1.56 (m, 2H), 1.63 (m, 2H), 1.74 (m, 2H), 2.38 (s, 3H), 3.24 (t, <sup>3</sup>J = 7.0 Hz, 2H), 3.93 (t, <sup>3</sup>J = 5.4 Hz, 1H). <sup>13</sup>C NMR (100 MHz, MeOH-*d*<sub>4</sub>): δ (ppm) = 24.2, 24.8, 28.3, 28.7, 29.7, 32.3, 39.9, 55.7, 157.8, 162.9, 172.3, 197.6. HR-MS: *m/z* 373.2333 (found); *m/z* 373.2338 (calcd for C<sub>18</sub>H<sub>33</sub>O<sub>6</sub>N<sub>2</sub> [M + H]<sup>+</sup>).

**N<sup>6</sup>-Pyruvoyl Lysine.** Compound 5 (590 mg, 1.59 mmol) was dissolved in acetone and 6 M HCl (10 mL each). After being stirred for 30 min, the mixture was diluted with 100 mL of water and concentrated to a volume of approximately 20 mL under a vacuum. After being washed with 20 mL of EtOAc, the aqueous phase was separated and evaporated to dryness. The crude product was purified by column chromatography on a Lichroprep RP C18 using water–methanol (9:1). Fractions with positive ninhydrin detections (TLC: R<sub>f</sub> 0.19 in water–butanol–acetic acid (8:1:1)) were collected, evaporated to dryness, and lyophilized to afford N<sup>6</sup>-pyruvoyl lysine as an orange amorphous material (302 mg, 88%). <sup>1</sup>H NMR (400 MHz, D<sub>2</sub>O): δ (ppm) = 1.42 (m, 2H), 1.61 (m, 2H), 1.90 (m, 2H), 2.43 (s, 3H), 3.26 (t, <sup>3</sup>J = 7.0 Hz, 2H), 3.82 (m, 1H). <sup>13</sup>C NMR (100 MHz, D<sub>2</sub>O): δ (ppm) = 22.7, 25.3, 28.7, 30.8, 39.7, 55.1, 163.1, 174.7, 199.1. HR-MS: *m/z* 217.1186 (found); *m/z* 217.1188 (calcd for C<sub>9</sub>H<sub>17</sub>O<sub>4</sub>N<sub>2</sub> [M + H]<sup>+</sup>).

**Aerated Incubations.** Mixtures containing N<sup>2</sup>-*t*-Boc-lysine (40 mM), phosphate buffer (0.1 M, pH 7.4), and either GO, MGO, ascorbic acid, the Amadori product, maltose, pyruvic acid, or glyoxylic acid (40 mM) were incubated in screw-cap vials. Incubations were done at 37 °C in a shaker for 7 days. Aliquots of 100 μL were collected each day and instantly stored at –20 °C until the analyses.

AGEs were analyzed by HPLC-MS<sup>2</sup> after the deprotection of the N<sup>2</sup>-*t*-Boc group. Pyruvic and glyoxylic acid formation were analyzed by GC-MS after silylation. Each sample was prepared at least three times.

**Deaerated Incubations.** The incubations were modified by using a phosphate buffer with 1 mM diethylenetriaminepentaacetic acid. The buffer was degassed with helium before the samples were placed in 0.7 mL screw-cap vials without air and incubated under an argon atmosphere.

**pH Incubations.** Aerated incubations were performed as described above, but the pH of the phosphate buffer was adjusted to 4.5 or 9.6 using 1 M HCl or NaOH.

**Housing of Animals and Induction of Cirrhosis by Carbon Tetrachloride (CCl<sub>4</sub>).** Male Wistar rats were used for all the experiments. The control and cirrhotic rats were bred in the Center of Medical Basic Research (ZMG), Medical Faculty, University of Halle, and the old rats were purchased from Janvier Laboratories (Le Genest-Saint-Isle, France). The rats were housed in standard cages in a climate room with 12 h light and dark phases and free access to food. The cirrhotic rats underwent inhalation exposure to CCl<sub>4</sub> three times a week. Phenobarbital (0.35 g/L) was added to the drinking water as described previously.<sup>23</sup> The treatment was given for 12 weeks. The livers were isolated 7–10 days after the last dose of CCl<sub>4</sub>. The principles for the care and use of animals from the American Physiological Society guide were followed. All animal experiments were approved by the local animal committee (42502-2-1123 MLU, Landesverwaltungsamt Sachsen-Anhalt, Germany).

**Tissue Collection.** The rats were anaesthetized with 150 mg/kg bodyweight narcoren (Merial, Lyon, France). In deep narcosis, the animals were killed by exsanguination, the livers were dissected after perfusion with Krebs-Ringer, and the samples were immediately snap-frozen. For the sirius-red staining, the livers were fixed in formaline (Histofix Roth, Karlsruhe, Germany) and processed routinely. For the Western blots, the livers were treated with a protein lysis buffer (RIPA) for the protein isolation. The primary antibodies were for vinculin (SC-5573, Santa Cruz Biotechnology, Dallas, Texas), α-SMA (ab5694), and TGF-β (ab66043, both abcam, Cambridge, UK). The

Table 1. Mass-Spectrometric Parameters for AGE Quantitation

AGE	retention time (min)	precursor		product ion 1 <sup>a</sup>			product ion 2 <sup>b</sup>			product ion 3 <sup>b</sup>		
		m/z (amu)	DP (V)	m/z (amu)	CE (eV)	CXP (V)	m/z (amu)	CE (eV)	CXP (V)	m/z (amu)	CE (eV)	CXP (V)
N <sup>6</sup> -carboxymethyl lysine	12.3	205.1	42	130.2	17	9	84.1	30	14	56.1	59	9
N <sup>6</sup> -glycoloyl lysine	12.2	205.2	40	142.1	20	11	84.1	36	14	56.2	64	8
N <sup>6</sup> -glyoxylyl lysine hydrate	11.7	221.1	40	203.3	15	13	140.1	25	12	157.3	19	12
N <sup>6</sup> -carboxyethyl lysine	17.8	219.1	54	130.1	18	11	84.1	33	7	56.1	59	8
N <sup>6</sup> -lactoyl lysine	16.2	219.2	40	156.2	20	8	84.1	35	9	173.1	17	8
N <sup>6</sup> -pyruvoyl lysine	19.5	217.0	55	154.0	19	12	84.1	32	6	171.0	15	12
N <sup>6</sup> -glycoloyl lysine-d1	12.2	206.2	40	143.1	20	11	84.1	36	14	160.1	64	8
N <sup>6</sup> -lactoyl lysine-d1	16.2	220.2	40	157.2	20	8	84.1	35	9	174.1	17	8

<sup>a</sup>MRM transition used for quantitation. <sup>b</sup>MRM transition used for confirmation.

Western-blot signals were quantified using a Fusion-Fx-7 imager with BD-Software (Peqlab, Erlangen, Germany).

**Protein Workup.** The protein was worked up by a modified procedure from Pogo et al.<sup>24</sup> Minced rat liver (250 mg) was weighed in a 14 mL round-bottom cell-culture tube (Greiner Bio-One, Kremsmuenster, Austria). Cooled (4 °C) lysis buffer (2 mL, 0.32 M sucrose, 3 mM MgCl<sub>2</sub>) was added, and the sample was lysed at 6500 rpm by an Ultra-Turrax (IKA, Staufen, Germany) for 2 min on ice. The lysate was cleared by 20 μm CellTrics filtration (Sysmex, Norderstedt, Germany) and centrifugation at 10 000 RCF for 15 min. The supernatant was separated, and 50% trichloroacetic acid (TCA) was added to a final concentration of 10%. The precipitate was washed twice with 5% TCA and isopropanol. After the precipitate was dried under a high vacuum, 3 mg of protein were dissolved in 1 mL of phosphate-buffered saline (PBS, pH 7.4, 150 mM NaCl, 10 mM phosphate) and homogenized by a MM 400 mixer mill (Retsch, Haan, Germany). After the addition of 200 μL of a NaBD<sub>4</sub> solution (15 mg/mL in 0.01 M NaOH), reduction was allowed to occur for 1 h at room temperature; then, the excess NaBD<sub>4</sub> was destroyed by 100 μL of 1 M HCl, and the solution was neutralized by 100 μL of 1 M NaOH. The samples were evaporated in a vacuum concentrator (Savant-Speed-Vac Plus SC 110 A combined with a Vapor Trap RVT 400, Thermo Fisher Scientific, Bremen, Germany), dissolved in water, and lyophilized. The lyophilizate was dissolved in 1 mL of PBS, and aliquots were used for the acid and enzymatic hydrolyses.

**Acid Hydrolysis.** The acid hydrolysis was performed as described by Glomb and Pfahler.<sup>13</sup> Aliquots of the protein solution (400 μL) were dried, and 800 μL of 6 M HCl was added. The solution was heated for 20 h at 110 °C under an argon atmosphere. The volatiles were removed in a vacuum concentrator, and the residue was dissolved in 492 μL of 0.05 M HCl. Prior to their injection into the HPLC-MS<sup>2</sup> system, the samples were filtered through 0.45 μm cellulose acetate Costar SpinX filters (Corning Inc., Corning, NY).

**Enzymatic Hydrolysis.** The enzymatic hydrolysis followed a slightly modified protocol by Smuda et al.<sup>5</sup> Pronase E (0.3 U, two additions), leucine aminopeptidase (1 U), and carboxypeptidase Y (0.95 U) were added to 500 μL aliquots of the protein solution. The enzymes were applied stepwise, and the incubations with each were for 24 h at 37 °C in a shaker incubator. A small crystal of thymol was added with the first digestion step. Once the total digestion procedure was completed, the reaction mixtures were filtered through 3000 Da molecular weight cutoff filters (VWR International, Radnor, PA).

For each sample, the efficiency of the acid hydrolysis was assigned to 100%, and the efficiency of the enzymatic hydrolysis was calculated by HPLC-MS<sup>2</sup> analysis of acid-stable CEL.

**Analytical HPLC-MS<sup>2</sup>.** A Jasco PU-2080 Plus quaternary gradient pump with a degasser and a Jasco AS-2057 Plus autosampler (Jasco, Gross-Umstadt, Germany) were used. The mass analyses were performed using an Applied Biosystems API 4000 quadrupole instrument (Applied Biosystems, Foster City, CA) equipped with an API source that used an electrospray-ionization (ESI) interface. The HPLC system was connected directly to the probe of the mass

spectrometer. Nitrogen was used as the sheath and auxiliary gas. To measure the analytes, the scheduled-multiple-reaction-monitoring (sMRM) mode of HPLC-MS<sup>2</sup> was used. The optimized parameters for the mass spectrometry are given in Table 1. The quantitation was based on the standard-addition method with known amounts of the pure authentic reference compounds. The values for the limits of detection (LOD) and limits of quantitation (LOQ) for the respective matrices are shown in Table 2.

Table 2. LODs and LOQs of AGEs in Incubations and Protein Hydrolysates

analyte	incubation		protein hydrolysate	
	LOD (mmol/mol lysine)	LOQ (mmol/mol lysine)	LOD (μmol/mol leucine)	LOQ (μmol/mol leucine)
N <sup>6</sup> -carboxymethyl lysine	0.040	0.121	0.777	2.590
N <sup>6</sup> -glycoloyl lysine	0.003	0.008	0.250	0.834
N <sup>6</sup> -glyoxylyl lysine hydrate	0.130	0.391	nd <sup>a</sup>	nd
N <sup>6</sup> -carboxyethyl lysine	0.019	0.058	0.413	1.375
N <sup>6</sup> -lactoyl lysine	0.003	0.011	0.071	0.238
N <sup>6</sup> -pyruvoyl lysine	0.009	0.028	nd	nd
N <sup>6</sup> -glycoloyl lysine-d1	nd	nd	0.144	0.481
N <sup>6</sup> -lactoyl lysine-d1	nd	nd	0.043	0.144

<sup>a</sup>nd = not determined.

**Model Incubations.** Prior to the injection into the HPLC-MS<sup>2</sup> system, 100 μL of 6 M HCl was added to 100 μL aliquots of the incubation solutions; the samples were kept at room temperature for 30 min and diluted on a scale of 1:10 with water.

Chromatographic separations were performed on a stainless-steel column (VYDAC 218TP54, 250 × 4.6 mm, RP18, 5 μm, Hesperia, CA) using a flow rate of 1 mL/min and a column temperature of 25 °C. The samples (10 μL) were injected at 2% B and run isocratically for 5 min. The gradient was changed to 100% B within 15 min (held for 10 min), and then the gradient was changed to 2% B within 5 min, at which it was held for 15 min. The eluents were ultrapure water (A) and a mixture of methanol and demineralized water (7:3, v/v; B), both of which were with 1.2 mL/L HFBA. sMRM mode was used for the mass-spectrometric detection.

**Protein Hydrolysates.** Chromatographic separations were performed on a stainless steel column (XSelect HSS T3, 250 × 3.0 mm, RP18, 5 μm, Waters, Milford, MA) using a flow rate of 0.7 mL/min and a column temperature of 25 °C. The samples (10 μL) were

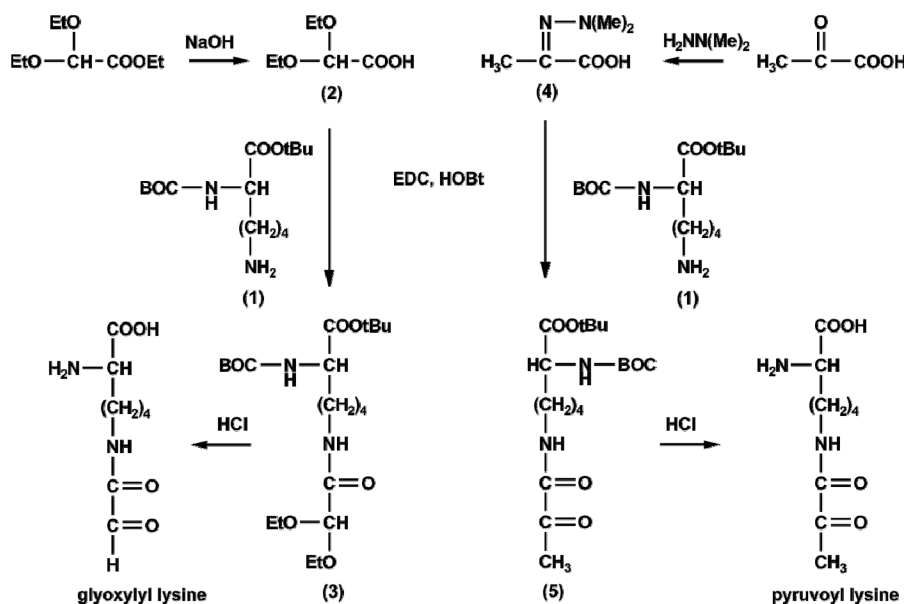


**Figure 1.** Synthesis of  $N^6$ -glyoxylyl lysine and  $N^6$ -pyruvoyl lysine.

injected at 2% B and run isocratically for 2 min. The gradient was changed to 14% B within 10 min (held for 0 min); 87% B within 22 min (held for 0 min); and 100% B within 0.5 min, at which it was held for 7 min. Then, the gradient was changed to 2% B within 2.5 min, at which it was held for 8 min. The eluents and mode were the same as described above.

**Ninhydrin Assay.** The ninhydrin assay was performed as described by Smuda et al.<sup>5</sup> After the complete workup, the contents of the amino acid modifications were standardized to that of L-leucine. A calibration of L-leucine, concentrated between 5 and 100  $\mu$ M, was performed and referenced to the diluted samples. Each sample was prepared four times.

**Analytical GC-MS.** The GC-MS method was established by Smuda et al.<sup>12</sup> The samples were analyzed on a Thermo Finnigan Trace GC Ultra coupled to a Thermo Finnigan Trace DSQ (both Thermo Fisher Scientific GmbH, Bremen, Germany). The GC column was a HP-5 (30 m  $\times$  0.32 mm, 0.25  $\mu$ m film thickness; Agilent Technologies, Palo Alto, CA), with an injector at 220  $^{\circ}$ C, a split ratio of 1:30, and a transfer line at 250  $^{\circ}$ C. The oven-temperature program was as follows: 100  $^{\circ}$ C (0 min), 7.5  $^{\circ}$ C/min to 200  $^{\circ}$ C (0 min), and 50  $^{\circ}$ C/min to 320  $^{\circ}$ C (10 min). Helium 5.0 was used as the carrier gas in constant-flow mode (linear velocity of 28 cm/s, flow of 1 mL/min). Mass spectra were obtained with EI at 70 eV (source: 210  $^{\circ}$ C) in selected-ion-monitoring mode: glyoxylic acid ( $m/z$  221.0/193.0/73.0) and pyruvic acid ( $m/z$  217.0/189.0/73.0). The retention times were as follows: glyoxylic acid was  $t_R$  = 5.85 min, and pyruvic acid was  $t_R$  = 4.00 min. Aliquots of the incubations (100  $\mu$ L) were dried in vacuo, the residues were dissolved in 100  $\mu$ L of pyridine, and 100  $\mu$ L of  $N,O$ -bis(trimethylsilyl)-acetamide with 5% trimethylchlorosilane was added. The samples were kept 4 h at 70  $^{\circ}$ C prior to injection into the GC-MS system.

**High-Resolution Mass Determination (HR-MS).** Positive-ion high-resolution ESI mass spectra were obtained from an Orbitrap Elite mass spectrometer (Thermo Fisher Scientific, Bremen, Germany) equipped with an HESI electrospray ion source (spray voltage of 4 kV, capillary temperature of 275  $^{\circ}$ C, source heater temperature of 40  $^{\circ}$ C, FTMS resolution >30,000). Nitrogen was used as the sheath and auxiliary gas. The sample solutions were introduced continuously via a 500  $\mu$ L Hamilton syringe pump with a flow rate of 5  $\mu$ L/min. The data were evaluated by the Xcalibur software 2.7 SP1.

**Nuclear-Magnetic-Resonance Spectroscopy (NMR).** NMR spectra were recorded either on a Varian VXR 400 spectrometer operating at 400 MHz for  $^1$ H and 100 MHz for  $^{13}$ C or on a Varian Unity Inova 500 instrument operating at 500 MHz for  $^1$ H and 125

MHz for  $^{13}$ C. SiMe<sub>4</sub> was used as the reference for calibrating the chemical shift.

**Statistical Analysis.** Analyses were performed in triplicate for each model incubation and resulted in coefficients of variation less than 5% for the AGE concentrations. All significance tests for the AGEs were performed by two-sample *t*-tests. Nonparametric tests (Kruskal–Wallis or Mann–Whitney) were used to detect differences between the groups for the markers of fibrosis.

## RESULTS AND DISCUSSION

**Syntheses of Authentic Reference Standards.**  $N^6$ -glyoxylyl lysine and  $N^6$ -pyruvoyl lysine were synthesized in an amide-coupling reaction catalyzed by EDC and HOBt (Figure 1). First, derivatives of glyoxylic acid and pyruvic acid with protected carbonyl functions were synthesized in order to increase their solubilities and prevent side reactions. Ethyl diethoxyacetate was treated with NaOH to yield glyoxylic acid diethoxy acetal, 2, which was coupled with 1 to give the fully protected amide 3. Pyruvic acid was protected as a  $N,N$ -dimethyl hydrazone, 4, and coupled with 1 to give the protected amide 5. The  $N,N$ -dimethyl hydrazone group had already been cleaved off during the silica gel chromatography, as described in literature.<sup>22</sup> Finally, amides 3 and 5 were deprotected by treatments with 3 M HCl to give  $N^6$ -glyoxylyl lysine and  $N^6$ -pyruvoyl lysine.

Both of the target compounds as well as the intermediates 2, 3, 4, and 5 were unequivocally verified by nuclear-magnetic-resonance (NMR) experiments and accurate mass determinations via HR-MS. Furthermore, the chemical shifts at 5.15 ppm in the  $^1$ H NMR experiments and 86.7 ppm in the  $^{13}$ C NMR experiments for the terminal aldehyde function showed that  $N^6$ -glyoxylyl lysine existed mainly as a hydrate. In contrast, the keto function of  $N^6$ -pyruvoyl lysine had a chemical shift of 199.1 ppm in the  $^{13}$ C NMR experiments, indicating its free carbonyl moiety.

**Formation of  $N^6$ -Glyoxylyl Lysine and  $N^6$ -Pyruvoyl Lysine.** The HPLC-MS<sup>2</sup> screenings of the aerated incubations of  $N^2$ -*t*-Boc-lysine, phosphate buffer and either glyoxal (GO), methylglyoxal (MGO), ascorbic acid, maltose, or the Amadori product of glucose and  $N^2$ -*t*-Boc-lysine under physiological conditions indicated the exclusive formation of  $N^6$ -glyoxylyl

lysine by GO and the formation of  $N^6$ -pyruvoyl lysine by MGO after 7 days at 37 °C. The time course of AGE formation was recorded by collecting aliquots every 24 h (Figure 2). After a 7

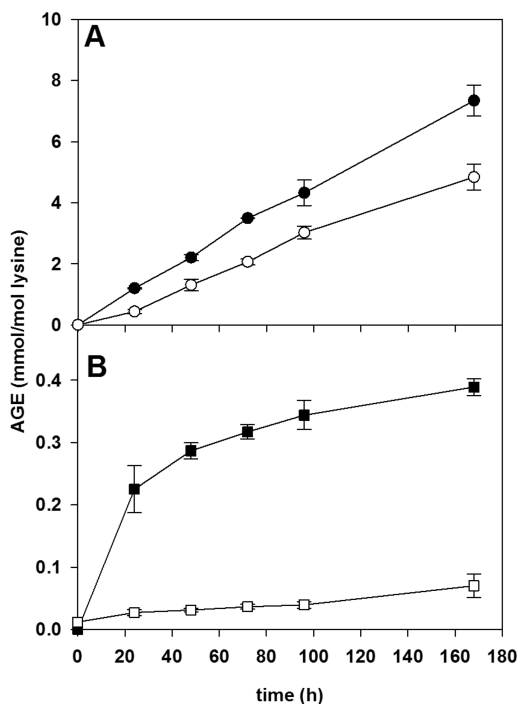


**Figure 2.** Formation of AGEs in incubations of  $N^6$ -*t*-Boc-lysine with glyoxal (A) or methylglyoxal (B) at 37 °C and pH 7.4 under aeration.  $N^6$ -Glycoloyl lysine (●),  $N^6$ -glyoxylyl lysine (○),  $N^6$ -lactoyl lysine (■), and  $N^6$ -pyruvoyl lysine (□).

day incubation, the molecular yield was 0.48 mol %  $N^6$ -glyoxylyl lysine and 0.01 mol %  $N^6$ -pyruvoyl lysine. Taking the short carbon chain of the precursors into account, a formation mechanism based on direct fragmentation of the educts was highly unlikely. Nevertheless, aliquots of the incubations were analyzed by GC-MS in order to determine the corresponding glyoxylic and pyruvic acids, which would be the main byproducts of any dicarbonyl-cleavage reaction.<sup>14</sup> No acid formation was monitored. This unequivocally excluded the formation of  $N^6$ -glyoxylyl lysine and  $N^6$ -pyruvoyl lysine by the

oxidative  $\alpha$ -dicarbonyl cleavage or amine-induced  $\beta$ -dicarbonyl cleavage of any putative reaction side-products resulting from, for example, aldol condensation. In addition, incubations of  $N^2$ -*t*-Boc-lysine with glyoxylic acid or pyruvic acid showed no formation of the corresponding amide AGEs, ruling out any mechanism of direct amide formation between the carboxylic acid function and the amine under the present conditions. The results therefore strongly pointed toward an isomerization-based reaction as the only possible source of  $N^6$ -glyoxylyl lysine and  $N^6$ -pyruvoyl lysine, which must include an oxidative step by definition. Consequently, the two novel amide AGEs should be alternative products of the established  $N^6$ -carboxymethyl lysine (CML)- and  $N^6$ -carboxyethyl lysine (CEL)-reaction cascades, which are based on isomerization (Figure 3).<sup>9</sup> The reaction starts with formation of the imine at one of the carbonyl functions (the keto function in the case of MGO, I). Hydration of the other carbonyl group allows the formation of an enamine, which rearranges to give the respective carboxyalkyl endproduct. If alternatively the isomerization starts from the hemiaminal intermediate (in the case of MGO at the aldehyde function, II) the respective  $\alpha$ -hydroxyamide endproducts result via an enaminol intermediate. Typically, the formation of the carboxyalkyl structure is favored by a factor of 5–30. Indeed, in the above model incubation, both structural classes were detected, reaching 0.73 mol %  $N^6$ -glycoloyl lysine (glycolic acid lysine amide, GALA) and 11.24 mol % CML in the case of GO, and 0.03 mol %  $N^6$ -lactoyl lysine and 0.12 mol % CEL in the case of MGO (Figure 2, data not shown for CML and CEL). This opened up the hypothesis that the novel  $\alpha$ -oxoamide AGEs,  $N^6$ -glyoxylyl lysine and  $N^6$ -pyruvoyl lysine, might stem from the direct oxidation of GALA and  $N^6$ -lactoyl lysine, respectively. However, this notion was undermined by an aerated incubation of the authentic  $\alpha$ -hydroxyamide references, where no oxidation products were detected after 7 days.

**Influence of Oxygen and pH.** Comparative incubations under aerated and deaerated conditions confirmed the nonoxidative pathway of CML, CEL, GALA, and  $N^6$ -lactoyl lysine formation, as there were almost no changes in their concentrations (Figure 4, aerated and deaerated 113 and 118 mmol/mol lysine, respectively, for CML; aerated and deaerated both 1.2 mmol/mol lysine for CEL). On the other hand,  $N^6$ -glyoxylyl lysine and  $N^6$ -pyruvoyl lysine were formed exclusively under aeration. This again stressed the need for an oxidation

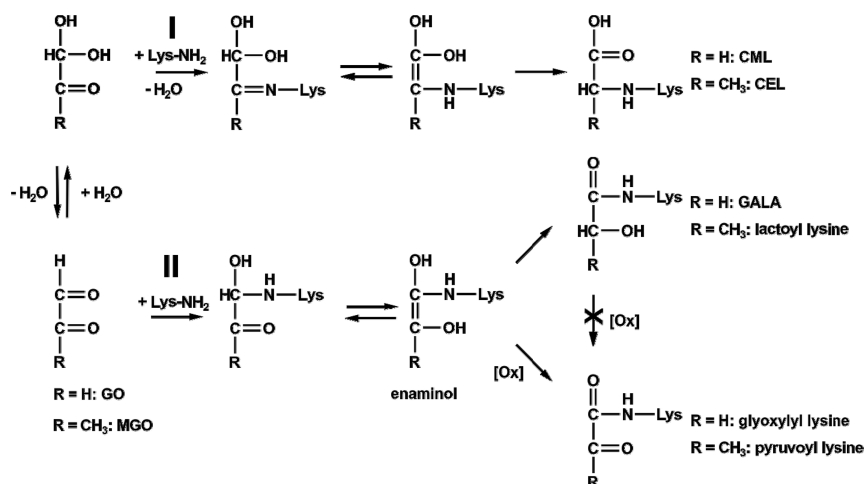


**Figure 3.**  $N^6$ -carboxymethyl lysine and  $N^6$ -carboxyethyl lysine isomerization reaction cascades.

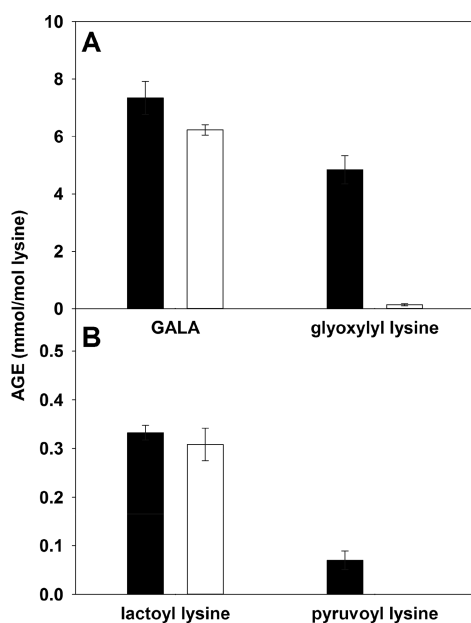


**Figure 4.** Effects of oxygen on the formation of AGEs in aerated (closed bars) and deaerated (open bars) incubations of  $N^2$ -*t*-Boc-lysine with glyoxal (A) or methylglyoxal (B) for 7 days at 37 °C and pH 7.4.

step within the isomerization-reaction scheme. The most likely electron-rich candidate is the enaminol (Figure 3), which should be readily oxidized to give the novel  $\alpha$ -oxoamide AGEs. In fact, Hofmann et al. described a similar enaminol intermediate in their explanation of the alternative formation of acids in the general Strecker degradation of amino acids. The nonoxidative degradation of the enaminol led to Strecker aldehydes, whereas in the presence of oxygen, the ratio significantly shifted from 4:1 to almost 1:2 toward the Strecker acids. However, because their setup was more related to food processing at high temperatures, they measured 0.83 mol % phenylacetaldehyde and 1.22 mol % phenylacetic acid in aerated incubations of glyoxal and phenylalanine after 60 min. In full support of our results, a direct oxidation of Strecker aldehydes to Strecker acids was ruled out by isotope-labeling experiments that pointed strongly toward the enaminol as the Strecker acid precursor.<sup>25</sup>

The CML- and CEL-reaction cascades were strongly dependent on pH values (Figure 5). In general, hardly any AGEs are formed under acidic conditions, because the  $N^6$ -amino function of lysine is protonated. This leads to a loss of nucleophilicity and prevents the necessary formation of Schiff base adducts. In contrast, the  $N^6$ -amino function is sufficiently deprotonated at pH 7.4 to allow an attack at the carbonyl carbon and initiate the formation of AGEs. A factor of about 100 was found between the yields of CML and CEL regardless of whether the reaction proceeded at pH 7.4 or 9.6. This must be attributed to the different character of the carbonyl function initiating the reaction. Whereas for CML, the  $N^6$ -amino group of the lysine attacks an aldehyde function of GO, CEL formation requires an attack at the much-less-reactive ketone moiety of MGO. On the other hand, the reason for the pronounced difference in the concentrations of GALA and  $N^6$ -lactoyl lysine and of  $N^6$ -glyoxylyl lysine and  $N^6$ -pyruvoyl lysine at pH 7.4 versus 9.6 by a factor of approximately 4 is less obvious. In diluted aqueous solutions, dicarbonyl structures exist predominantly in their hydrated forms; that is, GO almost

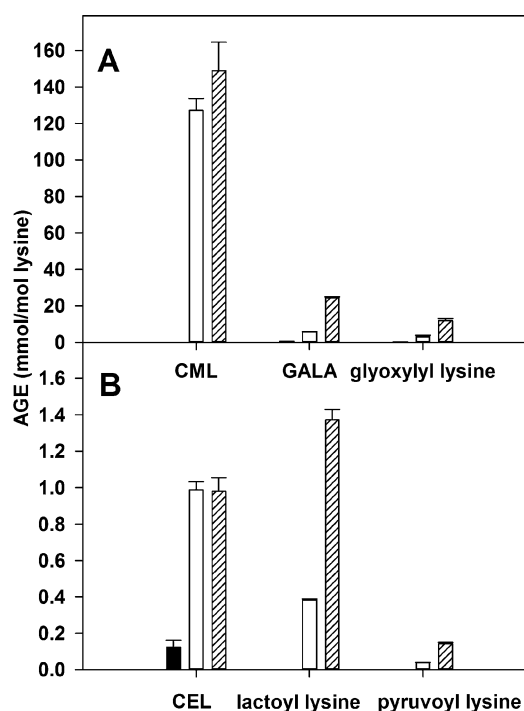


**Figure 5.** Effects of pH 4.5 (closed bars), 7.4 (open bars), and 9.6 (hatched bars) on the formation of AGEs in incubations of  $N^2$ -*t*-Boc-lysine with glyoxal (A) or methylglyoxal (B) for 7 days at 37 °C.

exclusively exists as the dihydrate,<sup>26</sup> and 56 and 44% of MGO exist in the mono- and dihydrated forms, respectively.<sup>27</sup> Although this does not change as a result of changes in the pH, the rate of enolization required for the rearrangement step does. This implies that the general course of the reaction is triggered mainly by two aspects, the stability of the endproducts and the rate of isomerization. Obviously in the case of CML and CEL, the high thermodynamic stabilities of the resulting carboxyalkyls are the main driving forces, resulting in almost no differences, whereas in the case of the  $\alpha$ -hydroxyamides and  $\alpha$ -oxoamides, pH-related changes in the kinetics of rearrangement prevail.

**Oxidative-Stress and Aging Markers.** Analyses of the AGEs in the model incubations were done after the acid hydrolysis of the BOC protection groups. As is apparent from the NMR data, there is an equilibrium between the carbonyl and hydrate forms. Consequently, HPLC separation led to very broad peaks with poor signal-to-noise ratios for the novel  $\alpha$ -oxoamide AGEs. This was especially pronounced for  $N^6$ -glyoxylyl lysine (LOD, 0.130 mmol/mol lysine; LOQ, 0.391 mmol/mol lysine) but still satisfactory for quantitation. However, the signals for the native  $\alpha$ -oxoamide AGEs were completely lost in the analyses of the liver-tissue samples because of the inevitable load of the matrix. In the first attempt to access the power of the novel AGEs as parameters of oxidative stress and aging, the soluble proteins of the rat livers were extracted by a lysis protocol. Because of their chemical natures, amide AGEs have to be released by enzymatic hydrolysis. The efficiency of this step was referenced to that of acid-stable CEL by a parallel acid-hydrolysis workup for each sample and was typically around 70–80%. Acid hydrolysis must include a reduction step with sodium borohydride to prevent any artifact formation, especially for CML. In the present study, the use of sodium borodeuteride allowed the differentiation of

$N^6$ -glyoxylyl lysine, in the form of  $N^6$ -glycoloyl lysine-d1, from any parallel-formed GALA and of  $N^6$ -pyruvoyl lysine, in the form of  $N^6$ -lactoyl lysine-d1, from  $N^6$ -lactoyl lysine. This also eliminated the chromatographic issues with the native  $\alpha$ -oxoamides and led to very sharp peaks and significantly reduced background noise. As a result, the sensitivity was improved by a factor of about 200 for  $N^6$ -glyoxylyl lysine (LOD, 0.144  $\mu\text{mol/mol}$  leucine; LOQ, 0.481  $\mu\text{mol/mol}$  leucine) and a factor of about 50 for  $N^6$ -pyruvoyl lysine (LOD, 0.043  $\mu\text{mol/mol}$  leucine; LOQ, 0.144  $\mu\text{mol/mol}$  leucine). The calculated concentrations of  $N^6$ -glyoxylyl lysine and  $N^6$ -pyruvoyl lysine were corrected by the subtraction of the natural-isotope peaks (10.16% of GALA and 11.17% of  $N^6$ -lactoyl lysine).

To test for the biological significance of the novel  $\alpha$ -oxoamides in aging, a rat model was chosen, and the AGEs were analyzed in the soluble-protein fraction of the liver. Inflammatory processes and oxidative stress in this organ were triggered by the induction of cirrhosis with tetrachloromethane. As shown in Table 3, the mean levels of all the AGEs

**Table 3.** AGEs in Soluble Proteins from Rat-Liver Lysates<sup>a</sup>

AGE ( $\mu\text{mol/mol}$ leucine)	3 month old (healthy)	3 month old (cirrhosis)	22 month old (healthy)
$N^6$ -carboxymethyl lysine	5.22 $\pm$ 3.34	5.40 $\pm$ 3.83	10.07 $\pm$ 7.01**
$N^6$ -glycoloyl lysine	0.73 $\pm$ 0.07	0.70 $\pm$ 0.09	1.36 $\pm$ 0.32**
$N^6$ -glyoxylyl lysine	0.37 $\pm$ 0.03	0.57 $\pm$ 0.16*	0.58 $\pm$ 0.03*
$N^6$ -carboxyethyl lysine	11.73 $\pm$ 2.32	8.34 $\pm$ 2.52	17.27 $\pm$ 4.35**
$N^6$ -lactoyl lysine	0.28 $\pm$ 0.06	0.34 $\pm$ 0.09	0.55 $\pm$ 0.06**
$N^6$ -pyruvoyl lysine	0.11 $\pm$ 0.04	0.23 $\pm$ 0.05*	0.27 $\pm$ 0.07*
markers of fibrosis (%)			
sirius-red staining	0.49 $\pm$ 0.14	23.16 $\pm$ 2.67*	1.70 $\pm$ 0.40*
TGF- $\beta$	100 $\pm$ 26	947 $\pm$ 661*	478 $\pm$ 143*
smooth muscle antigen	100 $\pm$ 31	1995 $\pm$ 1057*	453 $\pm$ 192*

<sup>a</sup>Means  $\pm$  standard deviations,  $n = 5$ . Significant differences were determined via the  $t$ -test or Mann–Whitney test by comparison with the AGE levels and markers of fibrosis in 3 month old healthy rats. \* $p < 0.05$ , \*\* $p < 0.001$ .

approximately doubled when 3 month and 22 month old rats were compared, showing  $p$  values  $< 5\%$  for  $N^6$ -glyoxylyl lysine and  $N^6$ -pyruvoyl lysine and  $< 0.1\%$  for all the other modifications. It is important to understand that GALA and  $N^6$ -glyoxylyl lysine are selective parameters for GO, whereas  $N^6$ -lactoyl lysine and  $N^6$ -pyruvoyl lysine are formed exclusively from MGO. On the other hand, CML can result not only from GO but also from many other precursors as glycolaldehyde or Amadori products. Taking the higher reactivity of GO and the various pathways leading to CML into account, it is quite surprising that the average CML levels in the aged rat livers (10.07  $\mu\text{mol/mol}$  leucine) were lower than the CEL levels (17.27  $\mu\text{mol/mol}$  leucine). A similar observation was found in the renal glomeruli of rats, in which CML was quantitated at 269  $\mu\text{mol/mol}$  lysine, and CEL was quantitated at 329  $\mu\text{mol/mol}$  lysine.<sup>28</sup>

When cirrhosis was induced, it was obvious that  $N^6$ -glyoxylyl lysine and  $N^6$ -pyruvoyl lysine were influenced not only by age but also by oxidative stress. Whereas all the other AGE parameters showed virtually no changes compared with the age-matched healthy control group, the two  $\alpha$ -oxoamides increased significantly ( $p < 5\%$ ). The prerequisite oxidation step in their

formation mechanism was already highlighted by the above  $N^2$ - $t$ -Boc-lysine model incubations. This implies that both of the parameters are indeed specific chemical markers for oxidative stress in vivo (Figure 6).

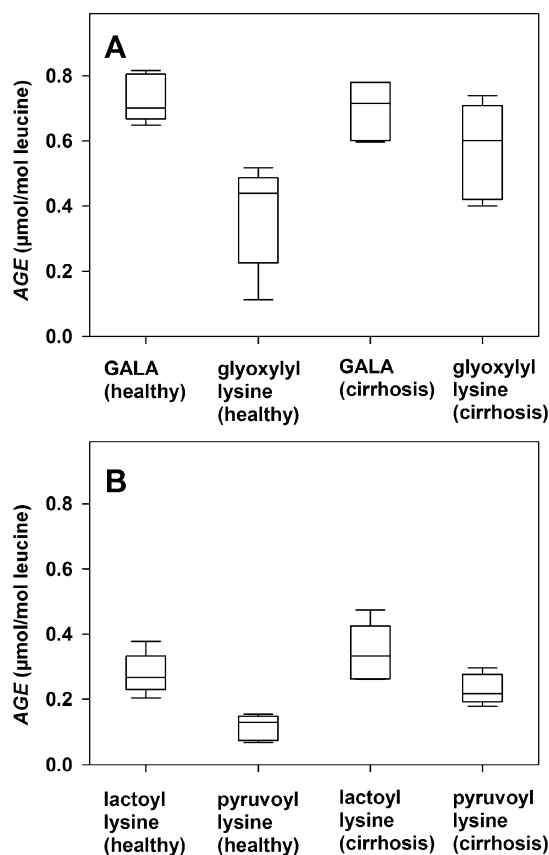


**Figure 6.** Correlation of GO-specific AGEs (A) and MGO-specific AGEs (B) in rat livers with cirrhosis. Black lines are median values.

The hypothesis of oxidative stress leading to  $\alpha$ -oxoamide formation was supported by sirius-red staining and Western blotting of transforming growth factor  $\beta$  (TGF- $\beta$ ) and  $\alpha$  smooth-muscle actin ( $\alpha$ -SMA, Table 3). Histological sirius-red staining of collagen is an established test for fibrosis, which is associated with increased oxidative stress.<sup>29</sup> Whereas collagen was nearly absent in the healthy, young rat livers (0.49%), fibrosis increased slightly with age (1.70%) and by a factor of about 50 in the cirrhotic animals (23.16%). Western blotting of TGF- $\beta$  and  $\alpha$ -SMA was another method used to access fibrosis-induced tissue changes. Additionally, TGF- $\beta$  signaling and expression as well as its activation from the latent complex are increased by reactive oxygen species, and TGF- $\beta$  itself in turn induces the production of reactive oxygen species.<sup>30</sup> The intensity of both markers was referenced as 100% for the young- and healthy-rat-liver proteins. In the 22 month old rats, the levels of TGF- $\beta$  (478%) and  $\alpha$ -SMA (453%) were nearly 5-times higher than they were in the young rats. The induction of fibrosis under oxidative stress was strongly accelerated in the cirrhotic rats, in which the TGF- $\beta$  levels elevated to 947%, and the  $\alpha$ -SMA levels elevated to 1995%. These results were thus in line with the significantly higher amounts of  $\alpha$ -oxoamides found in the old and cirrhotic rat livers.

To decouple the influences of aging and oxidative stress on the formation of  $\alpha$ -oxoamides, the ratios between GALA and

$N^6$ -glyoxylyl lysine and between  $N^6$ -lactoyl lysine and  $N^6$ -pyruvoyl lysine were calculated. Whereas the  $N^6$ -glyoxylyl/GALA and  $N^6$ -pyruvoyl/ $N^6$ -lactoyl lysine ratios remained on average constant at around 0.5 in the young and aged rat livers, the ratios in the cirrhotic livers increased to 0.8 for  $N^6$ -glyoxylyl/GALA and 0.7 for  $N^6$ -pyruvoyl/ $N^6$ -lactoyl lysine. These changes in the ratios may thus be valuable markers of liver cirrhosis in future research. Further investigations have to validate the present preliminary results and open up the applicability of these novel markers to other pathologies with inflammatory oxidative stress.

## AUTHOR INFORMATION

### Corresponding Author

\*E-mail: [marcus.glomb@chemie.uni-halle.de](mailto:marcus.glomb@chemie.uni-halle.de), Fax: ++049-345-5527341.

### ORCID

Tim Baldensperger: 0000-0002-9653-3156

Marcus A. Glomb: 0000-0001-8826-0808

### Funding

Funding was supported by the Deutsche Forschungsgemeinschaft (DFG, Germany) Research Training Group 2155, ProMoAge.

### Notes

The authors declare no competing financial interest.

## ACKNOWLEDGMENTS

We thank Dr. D. Ströhl from the Institute of Organic Chemistry, Halle, Germany, for recording the NMR spectra and Dr. A. Frolov from the Leibniz Institute of Plant Biochemistry, Halle, Germany, for performing the accurate mass determination.

## ABBREVIATIONS USED

AGEs, advanced-glycation endproducts; GO, glyoxal; MGO, methylglyoxal; CML,  $N^6$ -carboxymethyl lysine; CEL,  $N^6$ -carboxyethyl lysine; GALA,  $N^6$ -glycoloyl lysine; EDC, 1-ethyl-3-(3-(dimethylamino)propyl)carbodiimide; HOBt, hydroxybenzotriazole; TCA, trichloroacetic acid; PBS, phosphate-buffered saline; HFBA, heptafluorobutyric acid; sMRM, scheduled multiple-reaction monitoring; TGF- $\beta$ , transforming growth factor  $\beta$ ;  $\alpha$ -SMA,  $\alpha$  smooth-muscle actin

## REFERENCES

- (1) Maillard, L. C. Action des acidesamines sur les sucres: formation des melanoidines par voie methodique. *CR Acad. Sci. Paris* **1912**, 66–68.
- (2) Hellwig, M.; Henle, T. Baking, ageing, diabetes. A short history of the Maillard reaction. *Angew. Chem., Int. Ed.* **2014**, 53, 10316–10329.
- (3) Mottram, D. S.; Wedzicha, B. L.; Dodson, A. T. Acrylamide is formed in the Maillard reaction. *Nature* **2002**, 419, 448–449.
- (4) Delgado-Andrade, C. Carboxymethyl-lysine. Thirty years of investigation in the field of AGE formation. *Food Funct.* **2016**, 7, 46–57.
- (5) Smuda, M.; Henning, C.; Raghavan, C. T.; Johar, K.; Vasavada, A. R.; Nagaraj, R. H.; Glomb, M. A. Comprehensive analysis of maillard protein modifications in human lenses. Effect of age and cataract. *Biochemistry* **2015**, 54, 2500–2507.
- (6) Henning, C.; Liehr, K.; Girndt, M.; Ulrich, C.; Glomb, M. A. Extending the spectrum of  $\alpha$ -dicarbonyl compounds in vivo. *J. Biol. Chem.* **2014**, 289, 28676–28688.

- (7) Glomb, M. A.; Monnier, V. M. Mechanism of protein modification by glyoxal and glycolaldehyde, reactive intermediates of the Maillard reaction. *J. Biol. Chem.* **1995**, 270, 10017–10026.
- (8) Glomb, M. A.; Tschirmich, R. Detection of  $\alpha$ -Dicarbonyl Compounds in Maillard Reaction Systems and in Vivo. *J. Agric. Food Chem.* **2001**, 49, 5543–5550.
- (9) Henning, C.; Glomb, M. A. Pathways of the Maillard reaction under physiological conditions. *Glycoconjugate J.* **2016**, 33, 499–512.
- (10) Uchida, K.; Khor, O. T.; Oya, T.; Osawa, T.; Yasuda, Y.; Miyata, T. Protein modification by a Maillard reaction intermediate methylglyoxal. *FEBS Lett.* **1997**, 410, 313–318.
- (11) Davidek, T.; Robert, F.; Devaud, S.; Vera, F. A.; Blank, I. Sugar fragmentation in the Maillard reaction cascade. Formation of short-chain carboxylic acids by a new oxidative  $\alpha$ -dicarbonyl cleavage pathway. *J. Agric. Food Chem.* **2006**, 54, 6677–6684.
- (12) Smuda, M.; Voigt, M.; Glomb, M. A. Degradation of 1-deoxy-D-erythro-hexo-2,3-diulose in the presence of lysine leads to formation of carboxylic acid amides. *J. Agric. Food Chem.* **2010**, 58, 6458–6464.
- (13) Glomb, M. A.; Pfahler, C. Amides are novel protein modifications formed by physiological sugars. *J. Biol. Chem.* **2001**, 276, 41638–41647.
- (14) Smuda, M.; Glomb, M. A. Fragmentation pathways during Maillard-induced carbohydrate degradation. *J. Agric. Food Chem.* **2013**, 61, 10198–10208.
- (15) Smuda, M.; Glomb, M. A. Maillard degradation pathways of vitamin C. *Angew. Chem., Int. Ed.* **2013**, 52, 4887–4891.
- (16) Thorpe, S. R.; Baynes, J. W. CML. A brief history. *Int. Congr. Ser.* **2002**, 1245, 91–99.
- (17) Nowotny, K.; Jung, T.; Höhn, A.; Weber, D.; Grune, T. Advanced glycation end products and oxidative stress in type 2 diabetes mellitus. *Biomolecules* **2015**, 5, 194–222.
- (18) Fujioka, M.; Tanaka, M. Enzymic and Chemical Synthesis of e-N-(L-Propionyl-2)-L-Lysine. *Eur. J. Biochem.* **1978**, 90, 297–300.
- (19) Gellet, A. M.; Huber, P. W.; Higgins, P. J. Synthesis of the unnatural amino acid  $N\alpha$ -Ne-(ferrocene-1-acetyl)-l-lysine. A novel organometallic nuclease. *J. Organomet. Chem.* **2008**, 693, 2959–2962.
- (20) Pinto, A.; Conti, P.; Grazioso, G.; Tamborini, L.; Madsen, U.; Nielsen, B.; De Micheli, C. Synthesis of new isoxazoline-based acidic amino acids and investigation of their affinity and selectivity profile at ionotropic glutamate receptors. *Eur. J. Med. Chem.* **2011**, 46, 787–793.
- (21) Tapia, I.; Alcazar, V.; Moran, R. Synthesis of chromanes using pyruvic acid dimethylhydrazone dianion. *Can. J. Chem.* **1990**, 68, 2190–2191.
- (22) Katayama, H.; Utsumi, T.; Ozawa, C.; Nakahara, Y.; Hojo, H.; Nakahara, Y. Pyruvoyl, a novel amino protecting group on the solid phase peptide synthesis and the peptide condensation reaction. *Tetrahedron Lett.* **2009**, 50, 818–821.
- (23) Zipprich, A.; Loureiro-Silva, M. R.; Jain, D.; D'Silva, I.; Groszmann, R. J. Nitric oxide and vascular remodeling modulate hepatic arterial vascular resistance in the isolated perfused cirrhotic rat liver. *J. Hepatol.* **2008**, 49, 739–745.
- (24) Pogo, A. O.; Allfrey, V. G.; Mirsky, A. E. Evidence for increased DNA template activity in regenerating liver nuclei. *Proc. Natl. Acad. Sci. U. S. A.* **1966**, 56, 550–557.
- (25) Hofmann, T.; Münch, P.; Schieberle, P. Quantitative Model Studies on the Formation of Aroma-Active Aldehydes and Acids by Strecker-Type Reactions. *J. Agric. Food Chem.* **2000**, 48, 434–440.
- (26) Avzianova, E.; Brooks, S. D. Raman spectroscopy of glyoxal oligomers in aqueous solutions. *Spectrochim. Acta, Part A* **2013**, 101, 40–48.
- (27) McLellan, A. C.; Thornalley, P. J. Synthesis and chromatography of 1,2-diamino-4,5-dimethoxybenzene, 6,7-dimethoxy-2-methylquinoxaline and 6,7-dimethoxy-2,3-dimethylquinoxaline for use in a liquid chromatographic fluorimetric assay of methylglyoxal. *Anal. Chim. Acta* **1992**, 263, 137–142.
- (28) Thornalley, P. J.; Battah, S.; Ahmed, N.; Karachalias, N.; Agalou, S.; Babaei-Jadidi, R.; Dawnay, A. Quantitative screening of advanced glycation endproducts in cellular and extracellular proteins by tandem mass spectrometry. *Biochem. J.* **2003**, 375, 581–592.

(29) Moeller, M.; Thonig, A.; Pohl, S.; Ripoll, C.; Zipprich, A. Hepatic arterial vasodilation is independent of portal hypertension in early stages of cirrhosis. *PLoS One* **2015**, *10*, e0121229.

(30) Liu, R.-M.; Gaston Pravia, K. A. Oxidative stress and glutathione in TGF- $\beta$ -mediated fibrogenesis. *Free Radical Biol. Med.* **2010**, *48*, 1–15.